Statistical Study for Eigenfunctions of 1-dimensional Tight Binding Model

Wen-ge Wang[a,b] and Bambi Hu[a,c]
[a] Department of Physics and Centre for Nonlinear Studies, Hong Kong Baptist University, Hong Kong, China
[b] Department of Physics, South-east University, Nanjing 210096, China
[c] Department of Physics, University of Houston, TX77204, USA

For energy eigenfunctions of 1-dimensional tight binding model, the distribution of ratio of their nearest components, denoted by $f(p)$, gives information for their fluctuation properties. The shape of $f(p)$ is studied numerically for three versions of the 1D tight binding model. It is found that when perturbation is strong the shape of $f(p)$ is usually quite close to that of the Lorentzian distribution. In the case of weak perturbation the shape of the central part of $f(p)$ is model-dependent while tails of $f(p)$ are still close to the Lorentzian form.

PACS number 05.45.+b, 71.23.-k, 72.15.Rn

I. Introduction

Different versions of the one dimensional tight binding model with constant near-neighbor-hopping have attracted lots of attention for years (e.g., see [1,2]). Although these versions of the model has the common feature of Hamiltonian matrices being tridiagonal, they have been found showing distinct global behaviors such as localization and delocalization of energy eigenfunctions. For example, for the Anderson model [3] with random diagonal elements for the Hamiltonian matrix, localization can be established rigorously [4]. For the case of diagonal elements being quasi-periodic as in the 1D quasi-periodic tight binding model, both localized and extended wavefunctions have been found [2,5–7]. Recently, another interesting version of the model has also been studied. It has been found that, if some correlation is introduced into the diagonal elements of the Hamiltonian matrix of the Anderson model, delocalization can appear [8–12]. Clearly, global properties as localization and delocalization are not determined merely by the tridiagonal structure of the Hamiltonian matrices.

The main difference between the Anderson model and the quasi-periodic tight binding model lies in the global properties of the diagonal elements of their Hamiltonian matrices. More exactly, it lies in whether the diagonal elements are random or quasi-periodic (quasi-random). Since locally there is no difference between random and quasi-random numbers, one can expect that the difference between local statistical properties of energy eigenfunctions for the two models is not so distinct as that between their global behaviors.

Statistical properties of eigenfunctions have been studied extensively in recent years (for averaged shape see, e.g., [13–19], for fluctuations and correlations see, e.g., [16,20–23]). It is known that the Random Matrix Model (RMM) (see, e.g., [24,25]) and the Band Random Matrix Model (BRMM) (see, e.g., [26,27]) can be used to describe quantum chaotic systems and quasi-1D disordered models, respectively. Although one can expect that some features of the above mentioned 1D tight binding model may be described by the BRMM with band width equal to 1, due to the constant near-neighbor-hopping, it is impossible for all its important features to be able to be described by the BRMM (let alone RM). Therefore, when studying statistical properties of the 1D tight binding model one must keep in mind its peculiar features.

When studying statistical properties of energy eigenfunctions the first quantity coming to one's mind may be the distribution of the components c_i of the eigenfunctions. However, for the 1D Anderson model, due to the exponential decay of $|c_i|$ from its maximum, the distribution of c_i does not provide much information for local properties. On the other hand, the distribution of p_i, for the so-called Riccati variable $p_i \equiv c_i/c_{i-1}$, is related to both local and global properties of eigenfunctions [28]. In this paper we will study properties of this distribution.

This paper has the following structure. In section II, some properties of p_i are discussed. It is shown that $f(p)$, the distribution of p_i, not only gives information for local statistical properties of energy eigenfunctions, but also is related to a global property, the Lyapunov exponent. Tails of $f(p)$ are expected to behave as $1/p^2$ and in some cases the shape of $f(p)$ is expected to be close to the Lorentzian distribution. In section III, the shape of $f(p)$ is studied numerically for the Anderson model. It is shown that in the case of weak disorder most of $f(p)$ can be fitted quite well by the Lorentzian distribution. In the case of strong disorder, central parts of $f(p)$ deviate notably from the Lorentzian form and some features of $f(p)$ can be explained by perturbation theory. Section IV is devoted to a discussion about the shape of $f(p)$ for the other two versions of the 1D tight binding model mentioned above. Numerically, more or less similar results as for the Anderson model have been found for the two models. A brief conclusion and discussion are given in section V.

II. Properties of p_i

The Hamiltonian matrix of the 1D tight binding model is of the form

$$H_{ij} = \epsilon_i \delta_{ij} + v(\delta_{i,j+1} + \delta_{i,j-1}). \quad (1)$$

Without the loss of generality, we take $i, j = 0, 1, 2, \cdots N$. When N goes to infinity one has a chain of infinite length. Corresponding to the above mentioned three versions of the model, the site energies ϵ_i are random numbers, quasi-periodic numbers, and partly random numbers, respectively, distributed in the region $[-w/2, w/2]$. For the first and third versions flat distributions will be chosen. Without the loss of generality, we will take $w = 1$ in numerical calculations.

The stationary Schrödinger equation for eigenenergy E is

$$vc_{i+1} + vc_{i-1} + \epsilon_i c_i = Ec_i \quad (2)$$

with $c_k, k = i-1, i, i+1$, being components of the corresponding eigenfunction. Dividing both sides of Eq. (2) by vc_i, one can see that it is convenient to introduce another quantity $p_i \equiv c_i/c_{i-1}$, for which Eq. (2) becomes

$$p_{i+1} = \alpha_i - \frac{1}{p_i} \quad (3)$$

where

$$\alpha_i = \frac{E - \epsilon_i}{v}. \quad (4)$$

Notice that the value of p_1 is determined by Eq. (2) for $i = 0$ (c_{-1} does not exist), i.e., $p_1 = \alpha_0$. As a result, once the eigenenergy E is given, the eigenfunction can be obtained immediately from Eq. (3) for $i = 1, \cdots N-1$. Eq. (3) for $i = N$ (without p_{N+1} which does not exist), i.e., $p_N = 1/\alpha_N$, is the condition for E to be an eigenenergy. Conversely, one can also calculate the eigenfunction from $p_N = 1/\alpha_N$ and take $p_1 = \alpha_0$ as the condition for E to be an eigenenergy. In either way, even for an arbitrary value of E one can calculate a sequence of p_i from Eq. (3) (neglecting the last equation).

A relation between p_i and p_1 can be get from Eq. (3),

$$p_i = \frac{A_i p_1 + B_i}{A_{i-1} p_1 + B_{i-1}}, \quad (5)$$

where A_i and B_i are determined by recurrence relations

$$A_i = \alpha_{i-1} A_{i-1} - A_{i-2} \quad (6)$$

and

$$B_i = \alpha_{i-1} B_{i-1} - B_{i-2}, \quad (7)$$

respectively, with

$$A_2 = \alpha_1, \quad A_1 = 1 \quad (8)$$

and

$$B_2 = -1, \quad B_1 = 0. \quad (9)$$

(For more detailed properties of A_i and B_i, see Appendix A.)

For a sequence of p_i obtained from Eq. (3) for i from 1 to N, when N goes to infinity, one can calculate the distribution of p_i, denoted by $f(p)$. For a finite N, only a histogram can be obtained. For the top of the histogram to be close to a smooth function, N must be large. For brevity, we also use $f(p)$ to indicate the distribution for a finite sequence of p_i. The distribution $f(p)$ gives information for not only local fluctuation properties but also some global properties of eigenfunctions. For example, the Lyapunov exponent can be expressed as

$$\gamma(E) = \lim_{n\to\infty} \frac{1}{n} \ln |\frac{c_n}{c_0}| = \lim_{n\to\infty} \frac{1}{n} \sum_{i=1}^{n} \ln |p_i|$$

$$= \int f(p) \ln |p| dp. \quad (10)$$

As is known, for a localized eigenfunction, $|c_i|$ usually first increases (on average) exponentially and then decreases (on average) exponentially as i varies from 0 to N. Let us define the Lyapunov exponent for a finite sequence of p_i with i from $j+1$ to k as

$$\gamma(E, \beta) = \frac{1}{k-j} \ln |\frac{c_k}{c_j}| = \frac{1}{k-j} \sum_{i=j+1}^{k} \ln |p_i| \quad (11)$$

where β denotes the sequence of p_i. Denoting the sequence of p_i of the increasing part of the eigenfunction as β_+ and that of the decreasing part as β_-, one can see from Eq. (11) that $\gamma(E, \beta_+) > 0$ and $\gamma(E, \beta_-) < 0$. Clearly, $f_+(p)$, the distribution of p_i for β_+, and $f_-(p)$, the distribution of p_i for β_-, can not be equal to each other even when N goes to infinity. Therefore, when studying $f(p)$ distributions, there are three cases that should be distinguished, i.e., $f_+(p)$, $f_-(p)$ and $f_a(p) = (f_+(p) + f_-(p))$ for p_i in both β_+ and β_-. (In what follows we use $f(p)$ to denote all the three cases.)

Since it is difficult to study the shape of $f(p)$ analytically and directly, a related problem can be studied to gain some reasonable predictions for behaviors of $f(p)$. Suppose one has a set of p_1 with a distribution $F_1(p_1)$. Making use of Eq. (3), one can change p_1 to p_2 and obtain the distribution for p_2, denoted by $F_2(p_2)$. Proceeding this procedure, one can obtain the distribution for p_n, $F_n(p_n)$. As will be shown in Appendix B, $F_n(p_n)$ does not approach any fixed distribution when n goes to infinity, but their tails behave as $1/p^2$ and tails of $f(p)$ should also decay as $1/p^2$.

What is also worth mentioning here is that the Lorentzian distribution

$$f_L(p) = \frac{a/\pi}{(p-b)^2 + a^2} \tag{12}$$

with

$$b = \frac{\alpha_i}{2}, \qquad a = \sqrt{1-b^2}$$

is invariant under the change of the variable from p to $(\alpha_i - 1/p)$ when $|\alpha_i| < 2$. Since

$$\int_{-\infty}^{\infty} f_L(p) \ln|p| dp = 0 \tag{13}$$

(see Appendix B), it is impossible for $f_\pm(p)$ to be equal to $f_L(p)$ for localized states, while it is possible for $f_a(p)$. However, when $\gamma(E)$ is small, it is possible for $f_\pm(p)$ to be close to $f_L(p)$.

III. $f(p)$ for the Anderson model

In this section we study the form of $f(p)$ for the Anderson model by numerical calculations. First, in subsection A we discuss the methods for calculating $f(p)$. Then, in subsection B we study the shape of $f(p)$ for the case of weak disorder, i.e., when perturbation is strong. Finally, in subsection C the form of $f(p)$ is discussed for the case of strong disorder.

A. Methods for calculating $f(p)$

There are three methods for calculating $f(p)$ numerically. For the first method, one can try to find out eigenfunctions of a Hamiltonian matrix with N large enough for a good statistics for $f(p)$ obtained from the data of one energy eigenfunction. Since when diagonalizing large matrices the so-called QR method usually does not give correct results for long tails of eigenfunctions with very small $|c_i|$, we have used the following method to calculate eigenfunctions. First we chose an initial value E' and calculated $p_1, p_2, \cdots p_N$ by making use of Eq. (3) for $i = 0, 1, \cdots N-1$. Then, we changed E' to make p_N satisfy Eq. (3) for $i = N$ as exactly as possible, i.e., to reduce the value of $err = |(p_N - 1/\alpha_N)/p_N|$ as much as possible. As an example, when $v = 4.0$ and $N = 5 \times 10^5$, such an eigenfunction has been found with eigenenergy $E \approx -4.0044$. The value of err for this eigenfunction is about 10^{-14}. For this eigenfunction, $|c_i|$, on average, increases exponentially from $i = 0$ to $i = N$. The $f_+(p)$ distribution for this eigenfunction is given in Fig.1a (circles). The line in Fig.1a gives $f_-(p)$ for another eigenfunction with $E \approx -4.002$, for which $|c_i|$ decreases, on average, exponentially from $i = 0$ to $i = N$. This eigenfunction was obtained by calculating the sequence of $p_N, p_{N-1}, \cdots p_1$ and taking Eq. (3) for $i = 0$ as the condition for eigensolution. The value of eer for this eigenfunction is also about 10^{-14}. The shortcoming of this method is that it is difficult (if not impossible) to find out eigenfunctions for which both the increasing and decreasing (on average) parts of $|c_i|$ are large.

For the second method for calculating $f(p)$, one can diagonalize (many) Hamiltonian matrices with the same value of v but different realizations of the random diagonal elements. There are two restrictions for the dimension N of the matrices. One is that it must be large enough for eigenfunctions to be localized (exponentially decay). The other is that the QR method for diagonalization gives correct results for long tails of eigenfunctions. For eigenfunctions thus obtained with eigenenergies in a small energy region one can calculate a $f_a(p)$ distribution. The shortcoming of this method is that when v is large, in order to obtain localized eigenfunctions the dimension N of the matrices must also be large, which requires powful computers and long calculation time.

The third method is suggested by the fact that to obtain a sequence of p_i from Eq. (3) it is unnecessary for E to be an eigenenergy. In fact, when N is large enough, for any value of E one can calculate a $f_+(p)$ distribution ($\gamma(E)$ is positive). On the other hand, for $p'_i = 1/p_{N-i+1}$ one can get a sequence of p'_i corresponding to another realization of the random numbers and calculate a corresponding $f_-(p)$ distribution. Numerically, it has been found that when N is large enough the form of the $f(p)$ distributions thus obtained is not sensitive to the value of E, that is, whether E being an eigenenergy or not does not have any special influence on the form of $f(p)$. Therefore, for the purpose of studying the shape of $f(p)$, one does not need to calculate the exact eigenfunctions.

We have compared the above three methods numerically and found that they give the same results. Two comparisons between the second and third methods are given in Fig.2a and 2b, respectively, for the case of $v = 1.0$ and $v = 0.2$. In Fig.2a, the solid line represents $f_a(p)$ obtained by the third mothed for $E = -1.0$ (5×10^5 p_i have been calculated) and circles give $f_a(p)$ obtained by the second mothed of diagonalizing 30 Hamiltonian matrices with $N = 1000$. For each result of the diagonalizations 20 eigenfunctions with eigenenergies around -1.0 have been taken for calculating the $f_a(p)$. For the solid line and circles in Fig.2b, E is about -0.1, 2000 Hamiltonian matrices with $N = 250$ have been diagonalized and 10 eigenfunctions have been used for each matrix. The agreement between the two methods is quite clear in the figure. Since the third method is the most powerful and convenient, we will use it for the following calculations in this and the next sections.

B. Weak disorder

As mentioned in section II, $f_+(p)$ and $f_-(p)$ must be different for the Anderson model, since $\gamma(E, \beta)$ for the increasing and decreasing parts have different signs. However, in the case of weak disorder Lyapunov exponents $\gamma(E)$ are usually quite small. For example, when $v = 4.0$,

$\gamma(E \approx -4.0)$ is less than 1.0×10^{-3}. So it is possible for $f_+(p)$ to be close to $f_-(p)$. Indeed, Fig.1a shows that they are quite similar.

As discussed in section II, the Lorentzian distribution in Eq. (12) is a fixed distribution for the mapping in Eq. (3) and when $\gamma(E)$ is small $f_\pm(p)$ may be close to $f_L(p)$. Therefore, it is natural to fit the $f(p)$ distribution in Fig.1a by the Lorentzian distribution. Since $\overline{\alpha}_i$ in this case is $E/v \approx -1$, one can expect that parameters b and a for the Lorentzian distribution may be close to $\overline{\alpha}_i/2 \approx -0.5$ and $\sqrt{1-b^2} \approx 0.87$, respectively. Indeed, the best fit for the dots in Fig.1a by the Lorentzian distribution gives $b \approx -0.53$ and $a \approx 0.85$. The result is given in Fig.1b. It can be seen that the distribution $f_+(p)$ is indeed quite close to the Lorentzian form.

For the other values of E when $v = 4.0$, it has been found that when $|E|$ is larger than 0.2 and within the region for eigenenergies (roughly speaking $|E| < 2v$), the shapes of $f_\pm(p)$ can also be fitted quite well by the same Lorentzian distribution as for $E \approx -4$. When $|E|$ becomes less than 0.2, the top of $f(p)$ will gradually deviate from that of the Lorentzian form, while tails are still of the Lorentzian form as in Fig.1b. As an example, we present in Fig.3 central parts of $f_+(p)$ for $E = 0$ and its fitting curve of the Lorentzian form. For comparison, we have also given $f_+(p)$ distributions for $E = -4.0$, $E = -7.5$ and the corresponding fitting curves. The difference between $f_+(p)$ and $f_-(p)$ has also been studied for $0 < |E| < 0.2$ and has been found larger than that for the case of $|E| > 0.2$. When $E = 0$, $f_+(p)$ and $f_-(p)$ are almost the same. When $|E|$ becomes less than 0.2, the form of $f_a(p)$ will also gradually deviate from that of the Lorentzian distribution in the top region.

When the value of v is increased, similar numerical results have also been obtained for $|E| < 2v$. Particularly, in the case of v going to infinity (or, equivalently, letting w be zero while keeping v a constant), the shape of $f(p)$ can also be fitted quite well by the Lorentzian distribution except for some special values of E/v, e.g., 0 or -1, For these values of E/v some p_i are zero and the mapping in Eq. (3) can not procceed. But these special values are unimportant because they do not correspond to any eigensolution of the Hamiltonian matrix. Since when $w = 0$ eigenfunctions are extended and the Lyapunov exponents are zero, the form of $f(p)$ may be exactly the Lorentzian form when N goes to infinity.

When v is decreased from 4, deviation of $f_\pm(p)$ from the Lorentzian distribution will also appear in the region of large $|E|$. As v becomes smaller the region of deviation will become larger. For example, when $v = 2$ for most of the values of $|E| < 2v$ the shape of $f_\pm(p)$ can be fitted quite well by the Lorentzian form, but when $v = 1$ deviation of $f_\pm(p)$ from the Lorentzian form has been detected in the top region in most cases. Correspondingly when $v = 1$ obvious difference between $f_+(p)$ and $f_-(p)$ has also been found. Since $f_+(p)$ and $f_-(p)$ can compensate each other, $f_a(p)$ may be of a better Lorentzian form than $f_\pm(p)$. In deed, when $v = 1$ and $1.7 > |E| > 0.5$, the form of $f_a(p)$ has been found of a good Lorentzian form still in the top region.

The above phenomena for relatively small values of v can be explained by some results of the Appendix C. As shown there, an eigenfunction can be divided into perturbative and non-perturbative parts. For the perturbative part, Eqs. (C31) and (C32) tells that p_i behaves differently for the increasing and decreasing parts of the eigenfunction. Also as shown in Appendix C, when v becomes smaller the perturbative part will become larger, while for a fixed v eigenfunctions with large $|E|$ have larger perturbative parts than those with relatively small $|E|$. As a result, the difference between $f_+(p)$ and $f_-(p)$ will enlarge as v becomes smaller or $|E|$ becomes larger. Since some dynamical effects remain in $A_\alpha(j \to j+1)$, p_i of perturbative parts will also make $f_+(p)$ and $f_-(p)$ deviate from the Lorentzian distribution (cf. the next subsection).

C. Strong disorder

In the case of strong disorder (for small values of v), considerable difference between $f_+(p)$ and $f_-(p)$ has been found. An example is given in Fig.4 for $v = 0.2$ and $E = -0.1$, where the circles and the dashed line represent $f_+(p)$ and $f_-(p)$, respectively. Here $f_+(p)$ and $f_-(p)$ are distributions of p_i and $1/p_i$, respectively, obtained from Eq. (3). As discussed in section II and Appendix B, long tails of $f(p)$ should behave as $1/p^2$. In Fig.5a and 5b we show the above $f_+(p)$ and $f_-(p)$ distributions (dots) in logarithm scale and the corresponding fitting curves (solid lines) of the Lorentzian form for their tails. For the $f_+(p)$, due to the form of the central part, we can fit only one of its two tails by the Lorentzian distribution once. For the other tail similar fitting can also be done. It is quite clear from the figure that long tails of both $f_+(p)$ and $f_-(p)$ can be fitted well by the Lorentzian distribution.

In Fig.4 it can be seen that $f_+(p)$ changes only a little when p varies from -2 to 1. This can be explained by perturbation theory. In fact, Eq. (C31) in Appendix C shows that p_i for the perturbative part of an eigenfunction satisfies

$$p_j \approx \frac{1}{A_\alpha(j-1 \to j)} \tag{14}$$

where, according to Eq. (C18),

$$A_\alpha(j-1 \to j) = \frac{v}{E - \epsilon_{j-1}} + O(v^3). \tag{15}$$

To the first order of approximation, $p_j \approx (E - \epsilon_{j-1})/v$. So when v is small, the contribution of perturbative parts tends to make $f_+(p)$ close to a platform in the region of $p \in [(E-0.5)/v, (E+0.5)/v]$. Since there also exist

non-perturbative parts for which Eq. (14) does not hold and when v is not quite small higher order of approximation should also be considered, the region of the platform should be narrower. This can be seen quite clearly in Fig.6, in which $f_+(p)$ and $f_-(p)$ for $v = 0.1$ and $E = 0.1$ are presented.

IV. Two other versions of 1D tight binding model

A. Paired correlated Anderson model

When some correlation is introduced into the diagonal elements of the Hamiltonian matrix of the Anderson model, delocalization can appear. For example, one can arrange ϵ_i into pairs with $\epsilon_{2k} = \epsilon_{2k+1}$, where ϵ_{2k} for different pairs are random numbers [10]. In some energy regions, localization lengths for this model can be far larger than that for the corresponding standard Anderson model (for some special energies localization lengths may be infinite). But for local statistical properties as the shape of $f(p)$, it is reasonable to expect that the two models may show similar behaviors. In deed, similar properties as shown in section III for $f(p)$ of the Anderson model has also been found numerically for $f(p)$ of this model (Fig.7). Particularly, in the case of weak disorder, central parts of $f(p)$ for $|E|$ around zero can be fitted by the Lorentzian form better than for the corresponding case of the standard Anderson model (see Fig.7b compared with Fig.3c).

B. 1D quasi-periodic tight binding model

For this model, we take ϵ_i in Eq. (1) as

$$\epsilon_i = cos(2\pi i\sigma)/2 \tag{16}$$

where σ is an irrational number. Numerically it has been found that when v is large, e.g., $v \geq 4$, the form of $f(p)$ can by fitted quite well by the Lorentzian form (Fig.8a) when $E \neq 0$ and $f_+(p)$ is almost the same as $f_-(p)$ since eigenfunctions are extended. Even for quite small values of $|E|$, the fitting is also quite good. But when $E = 0$, $f(p)$ has a high peak in the neighbourhood of $p = 0$. Similar to the Anderson model, when v is decreased from 4, the form of $f(p)$ will deviate gradually from that of the Lorentzian distribution, especially for eigenfunctions with relatively large $|E|$. This is also due to the fact that for these eigenfunctions the perturbative parts become larger as v becomes smaller. In some cases it has been found that although $f_+(p)$ and $f_-(p)$ deviate from the Lorentzian form notably they are quite close to each other. When v is smaller than 1, many localized states can be found. For most of these localized states $f_+(p)$ have shapes much more irregular than that for the Anderson model. In Fig.8b we give an example for $v = 0.2$ and $E = -0.1$. Circles represent $f_+(p)$ and the solid line is the fitting curve of the Lorentzian form for the far right tail. The far left tail and the middle right tail (for p between 3 and 7) can also be fitted by the Lorentzian form but with different fitting parameters.

V. Conclusions and discussions

The distribution $f(p)$ of ratio of nearest components of energy eigenfunctions, $p_i = c_i/c_{i-1}$, is studied numerically in this paper for three versions of the 1-dimensional tight binding model: the Anderson model, a quasi-periodic tight binding model and a paired correlated Anderson model. It is shown that $f(p)$ for increasing and decreasing parts of eigenfunctions (denoted as $f_+(p)$ and $f_-(p)$, respectively) should be treated separately. Numerically the following results have been found for all the three models. (1) In the case of strong perturbation (weak disorder), when $|E|$ is not close to zero, $f_+(p)$ and $f_-(p)$ are close to each other and can be fitted quite well by the Lorentzian distribution. (2) In the case of weak perturbation (strong disorder), $f_+(p)$ deviates notably from $f_-(p)$ and only their tails can be fitted well by the Lorentzian distribution. Some features of the shape of $f_+(p)$ in the case of strong disorder for the Anderson model can be explained by perturbation theory.

Eq. (3) shows that once an energy E is given, $p_1, p_2, \cdots p_N$ can be calculated readily from the $i = 0, 1, \cdots N-1$ cases of the equation, despite of whether E is an eigenenergy or not (Eq. (3) for $i = N$ is the condition for E to be an eigenenergy). Numerically it has been found that E being an eigenenergy or not has no influence on whether $f(p)$ can be fitted well by the Lorentzian form. That is to say, the closeness between the distribution $f(p)$ and the Lorentzian distribution in the case of weak disorder is not specific for eigensolutions. It is in fact determined by the form of the mapping in Eq. (3). We would like to point out that this property of $f(p)$ is, in fact, related to a more general problem, that is, some information for properties of eigenfunctions may be obtained without diagonalizing the Hamiltonian matrix.

Acknowledgments

The authors are very grateful to Bao-wen Li, Guangshan Tian and Pei-qing Tong for valuable discussions. The authors are also thankful to J.M. Luck for introducing us to some previous related work on the Riccati variable. This work was partly supported by grants from the Hong Kong Research Grant Council (RGC), the Hong Kong Baptist University Faculty Research Grant (FRG), Natural Science Foundation of China and the National Basic Research Project "Nonlinear Science", China.

APPENDIX A: PROPERTIES OF A_I AND B_I

In order to express A_i and B_i explicitly by making use of $\alpha_1, \cdots, \alpha_i$, we first introduce a quantity $S_{ji}(0 < j < i)$ defined by

$$S_{ji} = \alpha_j \alpha_{j+1} \cdots \alpha_i. \tag{A1}$$

Taking out k pairs of neighbouring α_l arbitrarily from S_{ji}, one has a product of $(i-j+1-2k)$ $\alpha_{l'}$, denoted as $S_{ji}^{(km)}$. Let us define another quantity D_{ji} as

$$D_{ji} = S_{ji} - \sum_m S_{ji}^{(1m)} + \sum_m S_{ji}^{(2m)} - \cdots$$

$$= S_{ji} + (-1)^k \sum_{(k,m)} S_{ji}^{(km)}. \tag{A2}$$

Then, making use of Eq. (3) one can proof that

$$A_i = D_{1i}$$

$$B_i = -D_{2i} \tag{A3}$$

The following relations can be readily obtained from Eqs. (3), (A2) and (A3),

$$p_i = \frac{D_{ji} p_j - D_{(j+1)i}}{D_{j(i-1)} p_j - D_{(j+1)(i-1)}}, \tag{A4}$$

$$p_j = \frac{D_{(j+1)i} - p_i D_{(j+1)(i-1)}}{D_{ji} - p_i D_{j(i-1)}}. \tag{A5}$$

Eq. (5) is a special case of Eq. (A4). Conversely, p_1 can also be expressed as a function of p_i,

$$p_1 = \frac{p_i B_{i-1} - B_i}{A_i - p_i A_{i-1}}. \tag{A6}$$

Making use of Eq. (5) and then (A6), one has

$$p_1 p_2 \cdots p_{n-1} = A_{n-1} p_1 + B_{n-1}$$

$$= \frac{A_n B_{n-1} - A_{n-1} B_n}{A_n - p_n A_{n-1}}. \tag{A7}$$

On the other hand, from Eq. (A5) for $i = n$ and $j = 1, 2, \cdots, n-1$, the following relation can be obtained readily,

$$p_1 p_2 \cdots p_{n-1} = \frac{1}{A_n - p_n A_{n-1}}. \tag{A8}$$

Then, substituting Eq. (A8) into (A7) one has

$$A_n B_{n-1} - A_{n-1} B_n = 1. \tag{A9}$$

So for large $|A_n|$ and $|B_n|$, A_n/B_n is approximately a constant.

An interesting result of Eqs. (A9) and (5) for the case of large $|A_n|$ is that different p_1 gives approximately the same p_n. This means if $|A_n|$ approaches infinity when n goes to infinity, the distributions $f(p)$ for sequences start from different p_1 must be the same.

In principle, once A_i and B_i are known, explicit expressions for properties of the corresponding eigenfunction can be obtained. For example, from Eqs. (10) and (5), it can be seen that the Lyapunov exponent is determined by properties of A_n and B_n,

$$\gamma(E) = \lim_{n\to\infty} \frac{1}{n} \ln |A_n + \frac{B_n}{p_1}|. \tag{A10}$$

However, to obtain practically useful expressions for A_i and B_i from Eqs. (A2) and (A3) is mathematically quite difficult.

APPENDIX B: $F_N(P)$ AND $F_L(P)$

For a set of p_1 with some distribution $F_1(p_1)$, from probability theory (see, e.g., [29]) and Eq. (3) it is easy to find out the relation between $F_n(p_n)$ and $F_1(p_1)$

$$F_n(p_n) = (p_1 p_2 \cdots p_{n-1})^2 F_1(p_1)|_{p_n} \tag{B1}$$

where $p_1, p_2, \cdots, p_{n-1}$ on the right hand side are functions of p_n. From Eqs. (A6) and (A8), it can be found out that

$$F_n(p) = \frac{1}{(A_n - pA_{n-1})^2} F_1(\frac{pB_{n-1} - B_n}{A_n - pA_{n-1}}) \tag{B2}$$

where for simplicity the subscript of p_n has been omitted. Due to the fact that α_i is not a constant, $F_n(p)$ can not approach a fixed distribution as n goes to infinity.

The sum of $F_n(p)$,

$$F(p,n) \equiv \frac{1}{n} \sum_{i=1}^{n} F_i(p), \tag{B3}$$

is more important than $F_n(p)$, since it is just the average of the distributions $f(p)$ for p_i obtained from the set of p_1 by Eq. (3). Numerically it has been found that when $f(p)$ is close to $f_L(p)$ in Eq. (12), $F(p,n)$ first approaches $f_L(p)$ when n increases from $n = 1$, despite of which form $F_1(p_1)$ is. However, when n becomes larger than some quantities $F(p,n)$ will show quite large fluctuations if the Lyapunov exponent is positive. This is not difficult to understand since positive Lyapunov exponent makes $|A_n|$ increases exponentially and Eq. (B2) shows that $F_n(p)$ has peaks in a neighborhood of $q_n = A_n/A_{n-1}$ which becomes smaller as $|A_n|$ increases. Equation (B2) also shows that the form of F_1 has considerable influence on the form of $F_n(p)$ only in the neighborhood of q_n.

Out of the neighborhood, $F_n(p)$ behaves like $1/(p-q_n)^2$. Therefore, $F(p,n)$ (so $f(p)$) should behave as $1/p^2$ in the tail region.

In order to calculate the value of $\gamma = \int f_L(p) ln|p| dp$ for $f_L(p)$ in Eq. (12), we first change the variable to $q = \alpha_i - 1/p$, which gives

$$\gamma = \int_{-\infty}^{\infty} \frac{a/\pi}{(q-b)^2+a^2} ln|\frac{1}{\alpha_i - q}| dq. \tag{B4}$$

Then, changing q to $x = 2b - q$ we have

$$\gamma = -\int_{-\infty}^{\infty} \frac{a/\pi}{(x+b)^2+a^2} ln|x| dx. \tag{B5}$$

Finally, after changing x to $y = -x$ one can see that $\gamma = -\gamma$ which gives $\gamma = 0$.

APPENDIX C: PERTURBATIVE STUDY FOR 1D ANDERSON MODEL

In this appendix we study 1D Anderson model by making use of a generalization of the so-called Brillouin-Wigner perturbation expansion (GBWPE) [14]. According to GBWPE, when perturbation is not extremely strong, each eigenfunction can be divided into two parts, one of which can be expressed as a convergent perturbation expansion by making use of the other. For the former part, an expression for p_j will be given in this appendix, which is useful for understanding some features of the shape of $f(p)$ when perturbation is not strong.

For the 1D tight-binding model with Hamiltonian $H = H^0 + V$, we denote eigenstates of H^0 as $|k>$ and eigenstates of H as $|\alpha>$,

$$H^0|k> = E_k^0|k> \tag{C1}$$

$$H|\alpha> = E_\alpha|\alpha> . \tag{C2}$$

($E_k^0 = \epsilon_k$ in Eq. (1)) For the sake of completeness, we first give a brief discussion for the above mentioned GBWPE. Dividing the set of basis states $|k>$ into two parts denoted by S_P (including N_P basis states) and S_Q (including N_Q basis states), respectively, one has two projection operators

$$P \equiv \sum_{|k>\in S_p} |k><k|, \qquad Q \equiv 1 - P. \tag{C3}$$

Subspaces related to P and Q will be called in the following the P and Q *subspaces* , respectively. Splitting an arbitrary eigenstate $|\alpha>$ into two orthogonal parts $|\alpha> = |t> + |h>$ where $|t> \equiv P|\alpha>$ and $|h> \equiv Q|\alpha>$, it can be shown, by making use of the stationary Schrödinger equation, that

$$|\alpha> = |t> + \frac{1}{E_\alpha - H^0} QV|\alpha> . \tag{C4}$$

The iterative expansion of Eq. (C4) gives

$$|\alpha> = |t> + \frac{1}{E_\alpha - H^0} QV|t> + (\frac{1}{E_\alpha - H^0} QV)^2|t>$$

$$+ (\frac{1}{E_\alpha - H^0} QV)^3|t> + \cdots \tag{C5}$$

if

$$\lim_{n\to\infty} < T_\alpha^n | T_\alpha^n > = 0 \tag{C6}$$

where

$$|T_\alpha^n> \equiv (\frac{1}{E_\alpha - H^0} QV)^n |\alpha> . \tag{C7}$$

Here the eigenvalue E_α has been treated as a constant. Eq. (C5) is just the above mentioned *generalization of Brillouin-Wigner perturbation expansion (GBWPE)*. For convenience, in what follows let us use the following notations: $|i>$ denoting a basis state in the P subspace and $|j>$ denoting a basis state in the Q subspace. Then, Eq. (C5) gives

$$C_{\alpha j} \equiv < j|\alpha> = \sum_{i\in P} (\frac{V_{ji}}{E_\alpha - E_j^0} + \sum_{k\in Q} \frac{V_{jk}}{E_\alpha - E_j^0} \frac{V_{ki}}{E_\alpha - E_k^0}$$

$$+ \sum_{k,l\in Q} \frac{V_{jk}}{E_\alpha - E_j^0} \frac{V_{kl}}{E_\alpha - E_k^0} \frac{V_{li}}{E_\alpha - E_l^0} \cdots) C_{\alpha i} \tag{C8}$$

Generally to say, $< T_\alpha^n | T_\alpha^n >$ vanishes as $n \to \infty$ if P and Q subspaces are such chosen that, for any state $|j>$ in the Q subspace, $|E_\alpha - E_j^0|$ is large enough compared with V, i.e., if all the basis states $|k>$ with small $|E_\alpha - E_k^0|$ are in the P subspace. So there are generally many P (and correspondingly Q) subspaces ensuring the validity of Eq. (C5). In these P subspaces there exists one with the minimum number of basis states. Projection operators related to this P subspace and the corresponding Q subspace are denoted by P_m and Q_m, respectively. $|t_\alpha> \equiv P_m|\alpha>$ will be called in the following the *non-perturbative part* of $|\alpha>$, and $|h_\alpha> \equiv Q_m|\alpha>$ the *perturbative part*, which can be expressed in terms of $|t_\alpha>$, E_α, V and H^0 as shown in Eq. (C5). In what follows, we will discuss the P_m and Q_m subspaces only and for the sake of brevity we will omit the subscript m. It is clear from the above discussion that the subspace P will increase (correspondingly, Q will decrease) as the perturbation v becomes stronger. It can also be seen that for the Anderson model eigenfunctions with larger $|E - \overline{\epsilon_i}|$ have larger perturbative parts.

In order to study $C_{\alpha j}$ of the perturbative part of $|\alpha>$ in Eq. (C8), we make use of the concept of path, in

analogy to that in the Feynman's path integral theory [30]. For $(n+1)$ basis states $|k_0>, |k_1>, \cdots |k_{n-1}>, |k_n>$ with $|k_0>, \cdots |k_{n-1}>$ in the Q subspace and $|k_n>$ in either the Q or the P subspace, we term the sequence $k_0 \to k_1 \to \cdots \to k_{n-1} \to k_n$ *a path of n paces* from k_0 to k_n, if $V_{kk'}$ corresponding to each pace is non-zero. Clearly, paths from k_0 to k_n are determined by the structure of the Hamiltonian matrix in the H^0 representation. Attributing a factor $V_{kk'}/(E_\alpha - E_k^0)$ to each pace $k \to k'$, we define the contribution of a path s (from j to i) to $C_{\alpha j}$, denoted by $f_{\alpha s}(j \to i)$, as the product of the factors of all its paces. Then, $C_{\alpha j}$ in Eq. (C8) can be rewritten as

$$C_{\alpha j} = \sum_{i \in P} A_\alpha(j \to i) C_{\alpha i} \tag{C9}$$

where

$$A_\alpha(j \to i) = \sum_s f_{\alpha s}(j \to i) \tag{C10}$$

and s denotes possible paths from j to i.

An interesting property of $C_{\alpha j}$ given by Eq. (C8) is that they satisfy equations

$$\sum_k H_{jk} C_{\alpha k} = E_\alpha C_{\alpha j} \tag{C11}$$

even for arbitrary values of E_α and $C_{\alpha i}$. In fact, from the definition of $A_\alpha(j \to i)$ in Eq. (C10), it can be shown that

$$A_\alpha(j \to i) = \sum_{j' \neq j} \frac{V_{jj'}}{E_\alpha - E_j^0} A_\alpha(j' \to i) + \frac{V_{ji}}{E_\alpha - E_j^0}. \tag{C12}$$

Substituting Eq. (C12) into Eq. (C9), one has

$$C_{\alpha j} = \sum_{j' \neq j} \frac{V_{jj'}}{E_\alpha - E_j^0} C_{\alpha j'} + \sum_i \frac{V_{ji}}{E_\alpha - E_j^0} C_{\alpha i}, \tag{C13}$$

which gives Eq. (C11). Therefore, the values of E_α and $C_{\alpha i}$ must be determined by the other part of the eigenequation (C2), i.e., by equations for $C_{\alpha i}$,

$$\sum_k H_{ik} C_{\alpha k} = E_\alpha C_{\alpha i}, \tag{C14}$$

and the normalization condition (except for a common phase).

Now let us apply the above results to the study of the Hamiltonian in Eq. (1). Firstly, we discuss the case in which the value of v is so small that there is only one basis state $|k>$ satisfying $|E_\alpha - E_k^0| < v/2$. (For such a small perturbation strength Brillouin-Wigner perturbation expansion is also convergent.) In this case, the P subspace corresponding to the non-perturbative part of $|\alpha>$ is just this basis state $|k>$. Let us denote it by $|i>$. Then, for each $|j>$ in the Q subspace, according to Eq. (C9)

$$C_{\alpha j} = A_\alpha(j \to i) C_{\alpha i}. \tag{C15}$$

Due to the specific form of perturbation as shown in Eq. (1), paths starting from $j < i$ can never reach points $k > i$ and *vice versa*, i.e., paths can not cross "i". From the discussion of Eqs. (C11) and (C14), we know that $C_{\alpha j}$ given by Eq. (C15) satisfy Eq. (C11) naturally and the value of E_α is determined by the equation

$$v C_{\alpha i-1} + E_i^0 C_{\alpha i} + v C_{\alpha i+1} = E_\alpha C_{\alpha i} \tag{C16}$$

where $C_{\alpha i-1}$ and $C_{\alpha i+1}$, given by paths left to and right to i, respectively, are functions of E_α (see Eqs. (C15) and (C10)).

For simplicity, let us first discuss the case $j < i$. According to the definitions of $A_\alpha(j \to i)$ and $f_{\alpha s}(j \to i)$, one can find out that

$$A_\alpha(j \to i) = A_\alpha(j \to j+1) A_\alpha(j+1 \to i), \tag{C17}$$

where

$$A_\alpha(j \to j+1) = f_{\alpha s_1}(j \to j+1) + f_{\alpha s_2}(j \to j+1)$$

$$+ f_{\alpha s_3}(j \to j+1) + f_{\alpha s_4}(j \to j+1) + O(v^5). \tag{C18}$$

Paths s_1, s_2, s_3 and s_4 in Eq. (C18) are $s_1 : j \to j+1$, $s_2 : j \to j+1 \to j \to j+1$, $s_3 : j \to j+1 \to j+2 \to j+1$, and $s_4 : j \to j-1 \to j \to j+1$, respectively, and $O(v^5)$ represents the contribution of paths with more than 3 paces. Substituting Eq. (C17) into (C15), one has

$$p_{j+1} = \frac{C_{\alpha j+1}}{C_{\alpha j}} = \frac{1}{A_\alpha(j \to j+1)}; \tag{C19}$$

and

$$C_{\alpha j} = A_\alpha(j \to j+1) A_\alpha(j+1 \to j+2)$$

$$\cdots A_\alpha(i-1 \to i) C_{\alpha i}. \tag{C20}$$

Thus, on average,

$$C_{\alpha j} \approx (\overline{A})^{i-j} C_{\alpha i} \tag{C21}$$

where $\overline{A}$ is the average value of $A_\alpha(j \to j+1)$. From Eq. (C18) one can see that $|\overline{A}| < 1$, so $|C_{\alpha j}|$ increases exponentially as j approaches i. When $j > i$, similar arguments lead to the following relations

$$A_\alpha(j \to i) = A_\alpha(j \to j-1) A_\alpha(j-1 \to i), \tag{C22}$$

$$p_j = \frac{C_{\alpha j}}{C_{\alpha j-1}} = A_\alpha(j \to j-1) \tag{C23}$$

and

$$C_{\alpha j} \approx (\overline{A})^{j-i} C_{\alpha i}. \tag{C24}$$

Secondly, we discuss the case of v being larger than only a few $|E_\alpha - E_k^0|$. (This is a case in which Brillouin-Wigner perturbation expansions diverge.) In this case, the P subspace corresponding to the non-perturbative part of $|\alpha>$ is composed of more than one basis states with E_i^0 close to E_α distributed randomly in the region $[-w/2, w/2]$. Since N_p, the number of basis states in the P subspace, is much smaller than N, the total number of basis states, labels i are generally separated by labels j of $|j>$ in the Q subspace and there is generally no successive labels of i. On the other hand, S_Q, the set of $|j>$, is also separated into a series of subsets by $|i>$. For convenience, we denote the basis states $|i>$ in increasing order by $|i^{(1)}>, |i^{(2)}>, \cdots |i^{(q)}>, \cdots |i^{(N_P)}>$ with $i^{(1)} < i^{(2)} < \cdots < i^{(q)} \cdots < i^{(N_P)}$ and denote the corresponding series of subsets of S_Q by $S_Q^{(1)}, S_Q^{(2)}, \cdots S_Q^{(q)}, \cdots$.

To apply GBWPE to this case of perturbation strength, let us consider a state $|j>$ in $S_Q^{(q)}$ satisfying $i^{(q)} < j < i^{(q+1)}$. Due to the same reason as in the first case, paths starting from j can not cross $i^{(q)}$ and $i^{(q+1)}$, that is, they are restricted in the region $[i^{(q)}, i^{(q+1)}]$. Then, according to Eq. (C9)

$$C_{\alpha j} = A_\alpha(j \to i^{(q)}) \cdot C_{\alpha i^{(q)}} + A_\alpha(j \to i^{(q+1)}) \cdot C_{\alpha i^{(q+1)}}. \tag{C25}$$

Similar to Eq. (C17) in this case we have

$$A_\alpha(j \to i^{(q)}) = A_\alpha(j \to j-1) A_\alpha(j-1 \to i^{(q)})$$

$$A_\alpha(j \to i^{(q+1)}) = A_\alpha(j \to j+1) A_\alpha(j+1 \to i^{(q+1)}). \tag{C26}$$

Then,

$$C_{\alpha j} = A_\alpha(j \to j-1) \cdots A_\alpha(i^{(q)}+1 \to i^{(q)}) C_{\alpha i^{(q)}}$$

$$+ A_\alpha(j \to j+1) \cdots A_\alpha(i^{(q+1)}-1 \to i^{(q+1)}) C_{\alpha i^{(q+1)}} \tag{C27}$$

$$\approx (\overline{A})^{j-i^{(q)}} C_{\alpha i^{(q)}} + (\overline{A})^{i^{(q+1)}-j} C_{\alpha i^{(q+1)}}$$

Since only a few $|E_\alpha - E_i^0|$ for $|i>$ in the P subspace are smaller than v, Eq. (C18) also gives $|\overline{A}| < 1$.

There are N_P equations as Eq. (C14) which determine the value of E_α and give $(N_P - 1)$ relations between $C_{\alpha i}$. What is of special importance here is that E_α is determined mainly by one of these equations only. In fact, suppose $|C_{\alpha i^{(m)}}|$ is the largest one among $|C_{\alpha i}|$. For $j_m = i^{(m)} - 1$ and $j'_m = i^{(m)} + 1$, Eq. (C27) shows that both $C_{\alpha j_m}$ and $C_{\alpha j'_m}$ are mainly given by terms including $C_{\alpha i^{(m)}}$. From the discussions for Eqs. (C14) and (C16), one can see that E_α is mainly determined by equation,

$$E_\alpha - E_{i^{(m)}}^0 \approx v A_\alpha(j \to i^{(m)}) + v A_\alpha(j' \to i^{(m)}), \tag{C28}$$

i.e., by contribution of paths around $i^{(m)}$.

As a result, for any other state $|i>$ with $i = i^{(q)} \neq i^{(m)}$, it is generally impossible for both $C_{\alpha j}$ and $C_{\alpha j'}$ ($j = i-1$ and $j' = i+1$) to be mainly determined by terms including $C_{\alpha i}$. In fact, if that is possible, one will have an equation similar to Eq. (C28), which means that E_α is mainly determined by the contribution of paths around i. Generally, to say, this contradicts with Eq. (C28).

Then, at least one of $C_{\alpha j}$ and $C_{\alpha j'}$ should have a considerable contribution from the other $C_{\alpha i'}$ ($i' = i^{(q-1)}$ or $i' = i^{(q+1)}$). For example, Suppose $C_{\alpha j}$ has a considerable contribution from $C_{\alpha i'}$ with $i' = i^{(q-1)}$. This means $C_{\alpha j}$ is in the same order of magnitude as

$$(\overline{A})^{(i-i'-1)} C_{\alpha i'}$$

(see Eq. (C27)). Since according to the eigen-equation (C11)

$$v C_{\alpha i} = (E_\alpha - E_j^0) C_{\alpha j} - v C_{\alpha j-1}, \tag{C29}$$

one can see that $C_{\alpha i}$ is nearly in the same order of magnitude as $C_{\alpha j}$. Thus, for j_b satisfying $i > j_b > i'$ Eq. (C27) gives

$$C_{\alpha j_b} \approx (\overline{A})^{j_b - i'} C_{\alpha i'}. \tag{C30}$$

Similar result can also be obtained if $C_{\alpha j'}$ has a considerable contribution from $C_{\alpha i^{(q+1)}}$. Therefore, when k changes from $i^{(q)}$ to $i^{(q+1)}$ or from $i^{(q)}$ to $i^{(q-1)}$, $|C_{\alpha k}|$ should on average increase exponentially in at least one of the two cases. Specifically, if $i^{(q)} = 1$ for $q = 1$, $|C_{\alpha k}|$ should on average increase exponentially when k increases from $i^{(1)}$ to $i^{(2)}$. Similarly, for the case of $i^{(N_p)} = N$, $|C_{\alpha k}|$ should increase exponentially when k decreases from N to $i^{(N_p-1)}$.

Now it is easy to show that the eigenfunction of $|\alpha>$ should be localized. Let us start from the basis state $|1>$. If $|1>$ is in the P subspace, as discussed above, $|C_{\alpha k}|$ should on average increase exponentially when k changes from 1 to $i^{(2)}$. If $|1>$ is in the Q subspace, Eq. (C27) shows that $|C_{\alpha k}|$ also on average increases exponentially until k reaches the first $i = i^{(1)}$. Then, making use of the result of the above paragraph, it can be found that $|C_{\alpha k}|$ should increase exponentially as k changes from 1 to $i^{(m)}$. Similarly, it is easy to see that $|C_{\alpha k}|$ should on average decrease exponentially when k changes from $i^{(m)}$ to N. Thus, the eigenfunction of $|\alpha>$ has the property of exponential decay. Applying this result to Eqs. (C25) and (C26), one can found out the following relations

$$p_j \approx \frac{1}{A_\alpha(j-1 \to j)} \tag{C31}$$

and

$$p_j \approx A_\alpha(j \to j-1) \tag{C32}$$

for the increasing and decreasing parts of eigenfunctions, respectively.

Thirdly, let us increase the value of v further. In this case, there will be some successive labels i. That is to say, some of the subsets of S_P separated by S_Q may have more than one basis states $|i>$. When the numbers of basis states $|i>$ in the subsets of S_P are small compared with the numbers of basis states $|j>$ in the subsets of S_Q, following similar arguments as in the second step case one can see that when $|\overline{A}| < 1$ energy eigenfunctions should also be localized (exponential decay). Finally, when the number of basis states in S_P is larger than that in S_Q, exponential decay of eigenfunctions can not be proved by the method used above, but can be proved by other methods ([4]).

However, in these two cases the method is still useful for studying properties of p_j and two results can be obtained. First, for perturbative parts in a region of $j \in [j_1, j_2]$, if one of the values of $|C_{\alpha j_1}|$ and $|C_{\alpha j_2}|$ is far larger than the other, (C31) and (C32) can still be obtained from equations similar to Eqs. (C25) and (C26) Second, for $|E_\alpha| > w/2$, since larger $|E_\alpha|$ means larger $|E_\alpha - \epsilon_i|$, eigenfunctions with larger $|E_\alpha|$ have larger perturbative parts and so have more p_j satisfying Eqs. (C31) or (C32).

[1] D.J. Thouless, Phys. Rep. **13C**, 93 (1974).
[2] J.B. Sokoloff, Phys. Rep. **126**, 189 (1985).
[3] P.W. Anderson, Phys. Rev. **109**, 1492 (1958). E. Abrahams, P.W. Anderson, D.C. Licciardello and T.V. Ramakrishnan, Phys. Rev. Lett. **42**, 673 (1979).
[4] K. Ishii, Suppl. Prog. Theor. Phys. **53**, 77 (1973); F. Delyon, Y. Levy, and B. Soulliard, Phys. Rev. Lett. **55**, 618 (1985); B. Simon, M. Taylor and T. Wolff, ibid. **54**, 1589 (1985), and references therein.
[5] S. Aubry and C. André, Proc. Israel Physical Society, ed. C.G. Kuper 3 (Adam Hilger, Bristol, 1979) p. 133.
[6] C.M. Soukoulis and E.N. Economou, Phys. Rev. Lett. **48**, 1043 (1982).
[7] H. Hiramoto and M. Kohmoto, Int. J. Mod. Phys. **B6**, 281 (1992).
[8] J.C. Flores, J. Phys. Condens. Matter, **1**, 8471 (1989).
[9] D.H. dunlap, H-L. Wu and P.W. Phillips, Phys. Rev. Lett. **65**, 88 (1990).
[10] J. Heinrichs, Phys. Rev. B **51**, 5699 (1995).
[11] A. Sánchez, F. Dominguez-Adame and E. Maciá, Phys. Rev. B **51**, 173 (1995).
[12] S.N. Evangelou and A.Z. Wang, Phys. Rev. B **47**, 13126 (1993).
[13] G. Casati, B.V. Chirikov, I. Guarneri and F.M. Izrailev, Phys. Lett., **A 223**, 430 (1996).
[14] Wen-ge Wang, F.M. Izrailev and G. Casati, Phys. Rev. E **57**, 323 (1998).
[15] V.V. Flambaum, A.A. Gribakina, G.F. Gribakin, and M.G. Kozlov, Phys. Rev. A **50**, 267 (1994).
[16] G. Casati, V.V. Flambaum and F.M. Izrailev, " Structure of eigenstates and local spectral density of states: Wigner band random matrix model ", (1997) preprint.
[17] F. Borgonovi, I. Guarneri, F.M. Izrailev and G. Casati, " Chaos and Thermalization in a Dynamical Model of Two Interacting Particles", (1997) preprint.
[18] V.Zelevinsky, B.A. Brown, N. Frazier, and M. Horoi, Phys. Rep., **276**, 85 (1996).
[19] V.V. Flambaum and F.M. Izrailev, Phys. Rev. E **56**, 5144 (1997).
[20] B. Eckhardt, Phys. Rep. **163**, 205 (1987), and references there in.
[21] Xu Gong-ou, Gong Jiang-bin, Wang Wen-ge, Yang Yatian and Fu De-ji, Phys. Rev. E **51**, 1770 (1995).
[22] V.N. Prigodin, Phys. Rev. Lett., **74** (1995) 1566. V.N. Prigodin, N. Taniguchi, A. Kudrolli, V. Kidambi, and S. Sridhar, Phys. Rev. Lett., **75** (1995) 2392.
[23] S. Hortikar and M. Srednicki, Phys. Rev. Lett., **80** (1998) 1646.
[24] M.L. Mehta, Random Matrices (Academic Press, San Diego, Second Edition, 1991).
[25] T. Guhr, A. Müller-Groeling and H.A. Weidenmüller, "Random Matrix Theories in Quantum physics: Common Concepts", cond-mat/9707301.
[26] Y.V. Fyodorov and A.D. Mirlin, Int. J. Mod. Phys., **8**, 3795 (1994).
[27] F.M. Izrailev, Chaos, Solitons & Fractals **5**, 1219 (1995).
[28] C. Barnes and J.M. Luck, J. Phys. A **23**, 1717 (1990). J.M. Luck, Systèmes Désordonnés Unidimensionnels, 209 pages, Collection Aléa Saclay, 1992.
[29] G.P. Beaumont, Probability and Random Variables (Ellis Horwood Limited, Chichester, 1986).
[30] R.P. Feynman and R.G. Hibbs, Quantum mechanics and path integrals, McGraw-Hill, New York, 1965.

FIG. 1. (a) A comparison (in logarithm scale) between the distribution $f_+(p)$ for an increasing eigenfunction with $E \approx -4.0044$ (circles) and the $f_-(p)$ for a decreasing eigenfunction with $E \approx -4.002$ (solid line) when $v = 4.0$ and $N = 5 \times 10^5$ for the Anderson model. (b) $f_+(p)$ in (a) and the fitting curve of the Lorentzian form

FIG. 2. Comparisons between $f_a(p)$ obtained by the second method of diagonalizing many Hamiltonian matrices (circles) and that by the third method of making use of Eq. (3) (solid lines) for (a) $v = 1.0, E = -1.0$ and (b) $v = 0.2, E = -0.1$.

FIG. 3. Central parts of $f_+(p)$ (circles) for the Anderson model and the fitting curves (solid lines) of the Lorentzian form for $v = 4.0$ and (a) $E = -7.5$, (b) $E = -4.0$, (c) $E = 0$.

FIG. 4. Central parts of $f_+(p)$ (circles) and $f_-(p)$ (dashed line) for $v = 0.2$ and $E = -0.1$ for the Anderson model.

FIG. 5. (a) The fitting curve (solid line) of the Lorentzian form for the left tail (dots) of the $f_+(p)$ in Fig.4 (in logarithm scale). (b) Same as (a) for tails of the $f_-(p)$ in Fig.4.

FIG. 6. Central parts of $f_+(p)$ (circles) and $f_-(p)$ (dashed line) for $v = 0.1$ and $E = 0.1$ for the Anderson model.

FIG. 7. Central parts of $f_+(p)$ (circles) for the paired correlated Anderson model and the fitting curves (solid lines) of the Lorentzian form for $v = 4.0$ and (a) $E = -4.0$, (b) $E = 0$.

FIG. 8. $f_+(p)$ (circles) for the 1D quasi-periodic tight binding model and the fitting curves (solid lines) of the Lorentzian form. (a) $v = 4.0, E = -4.0$, (b) $v = 0.2, E = -0.1$ and the fitting curve is for the far right tail only.

Fig.1

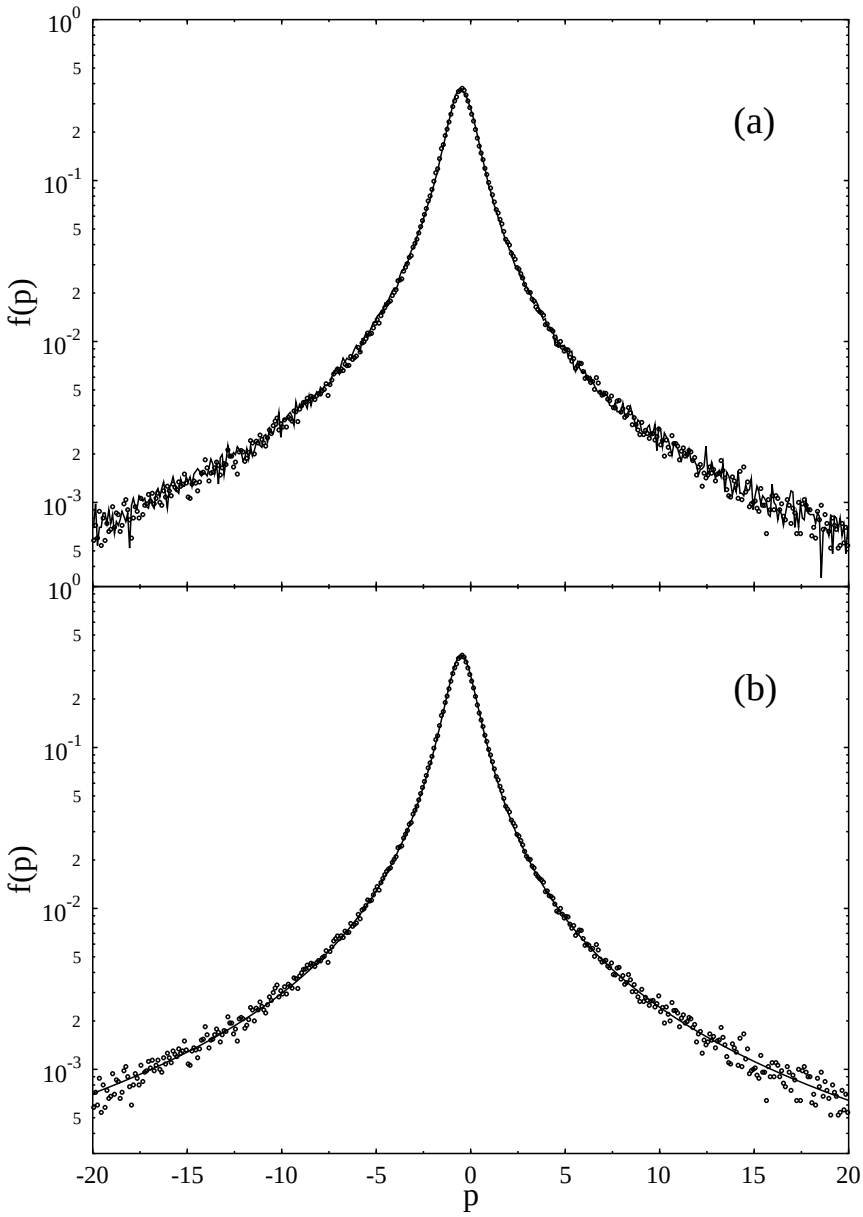

Fig.2

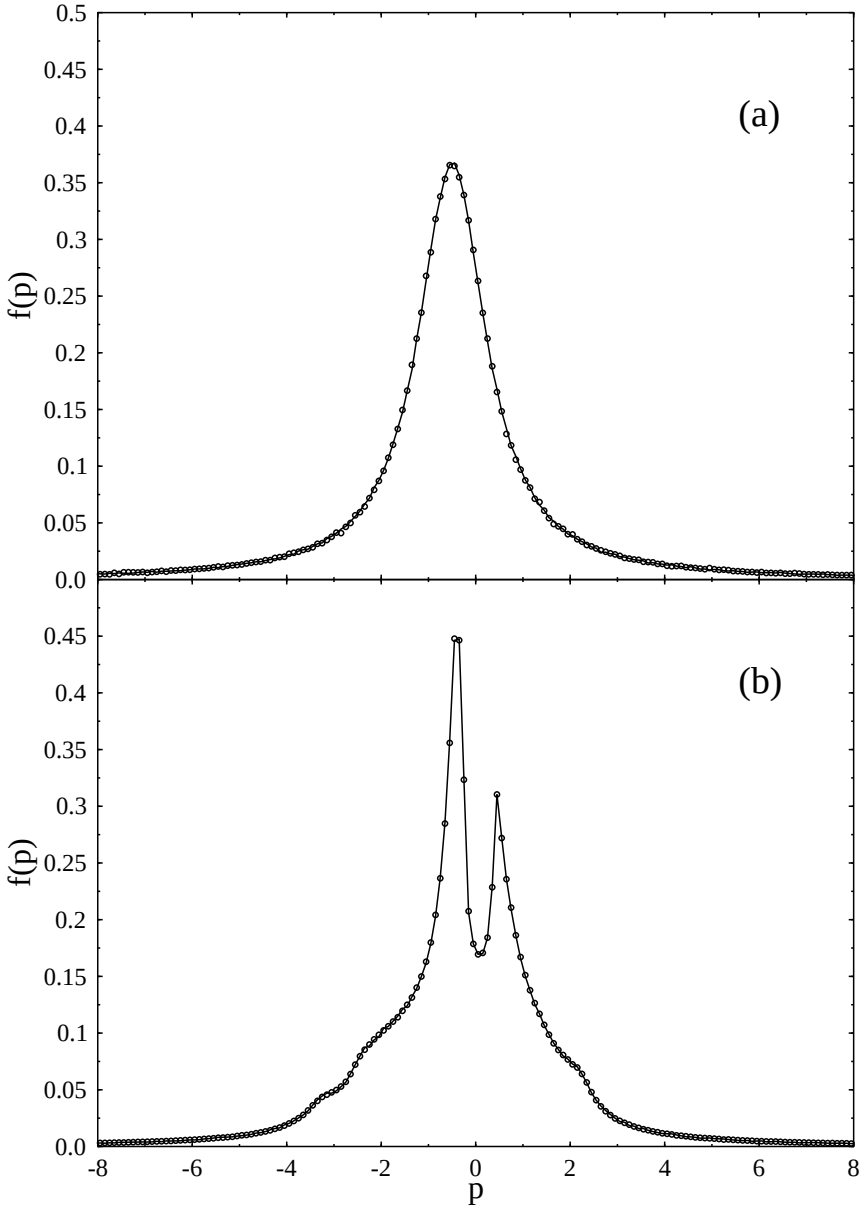

Fig.3

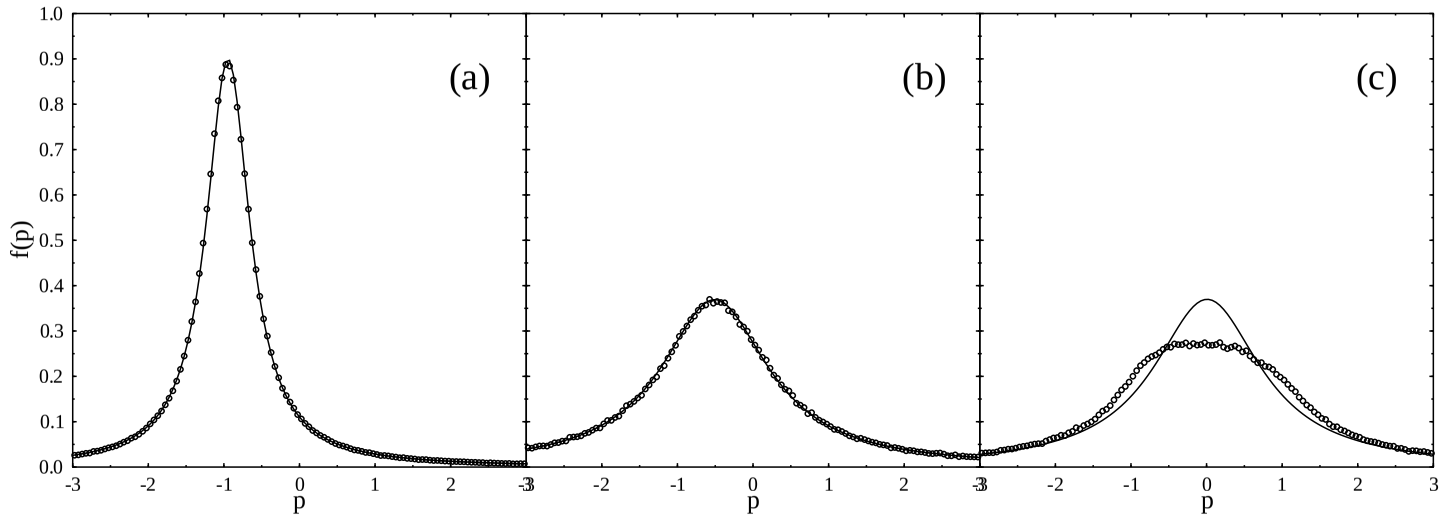

Fig.4

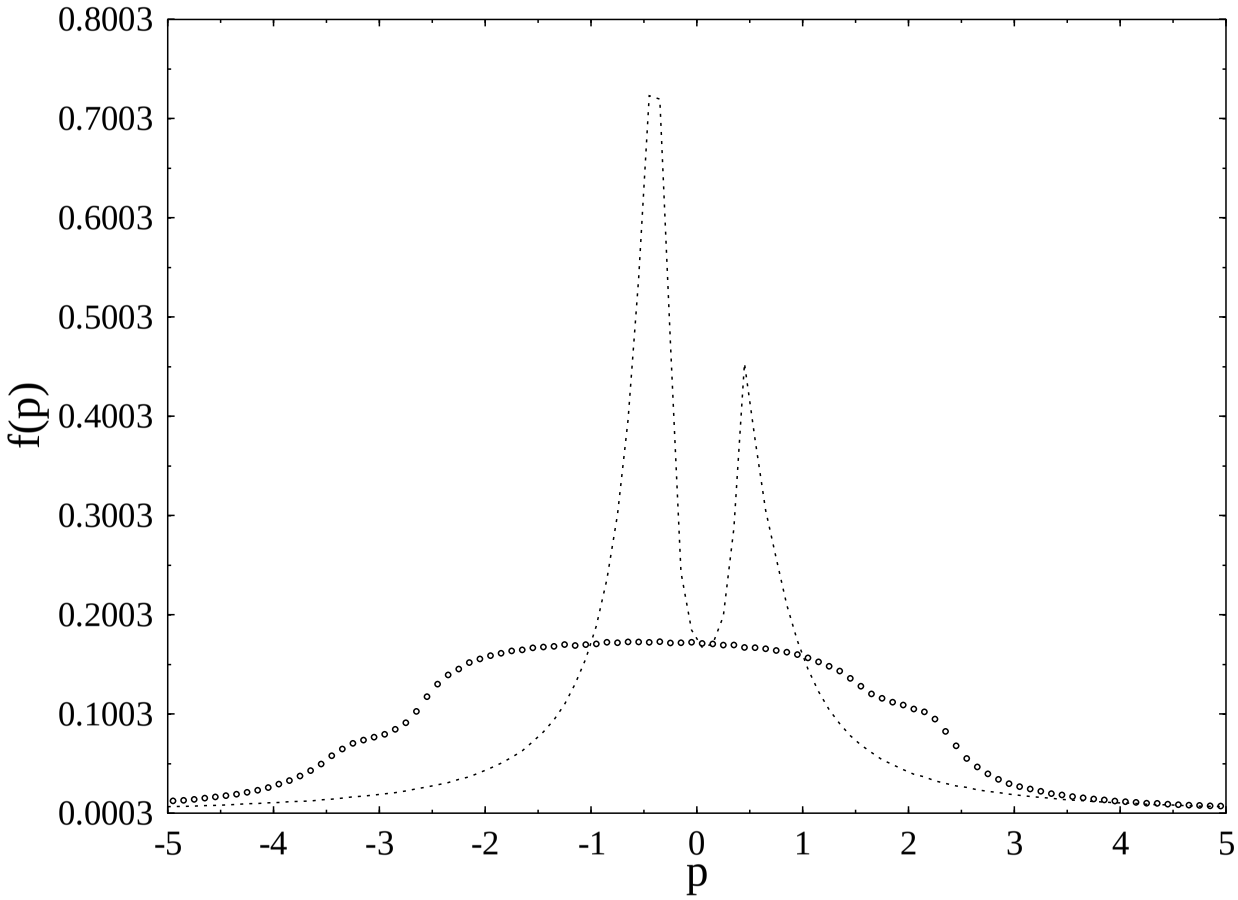
0.8003
0.7003
0.6003
0.5003
0.4003
0.3003
0.2003
0.1003
0.0003
f(p)
-5
-4
-3
-2
-1
0
1
2
3
4
5
p

Fig.5

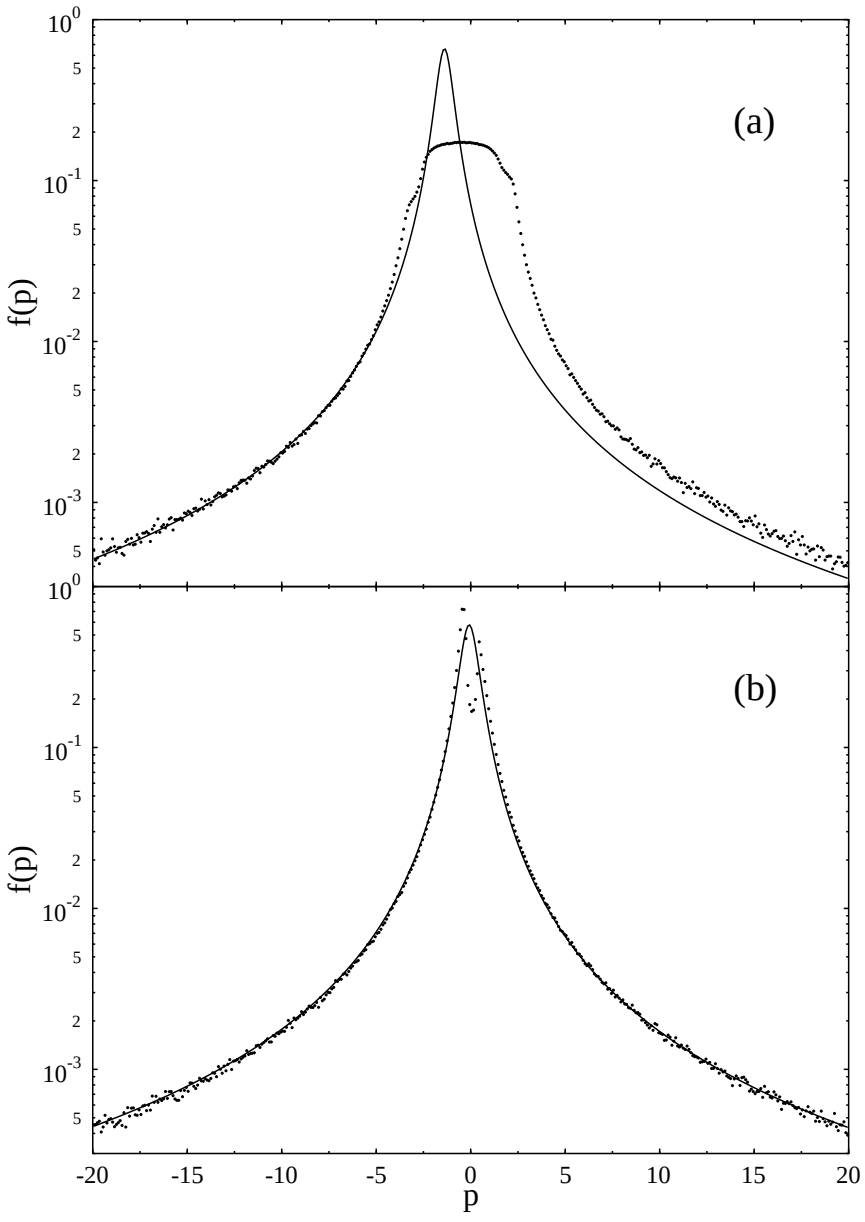

Fig.6

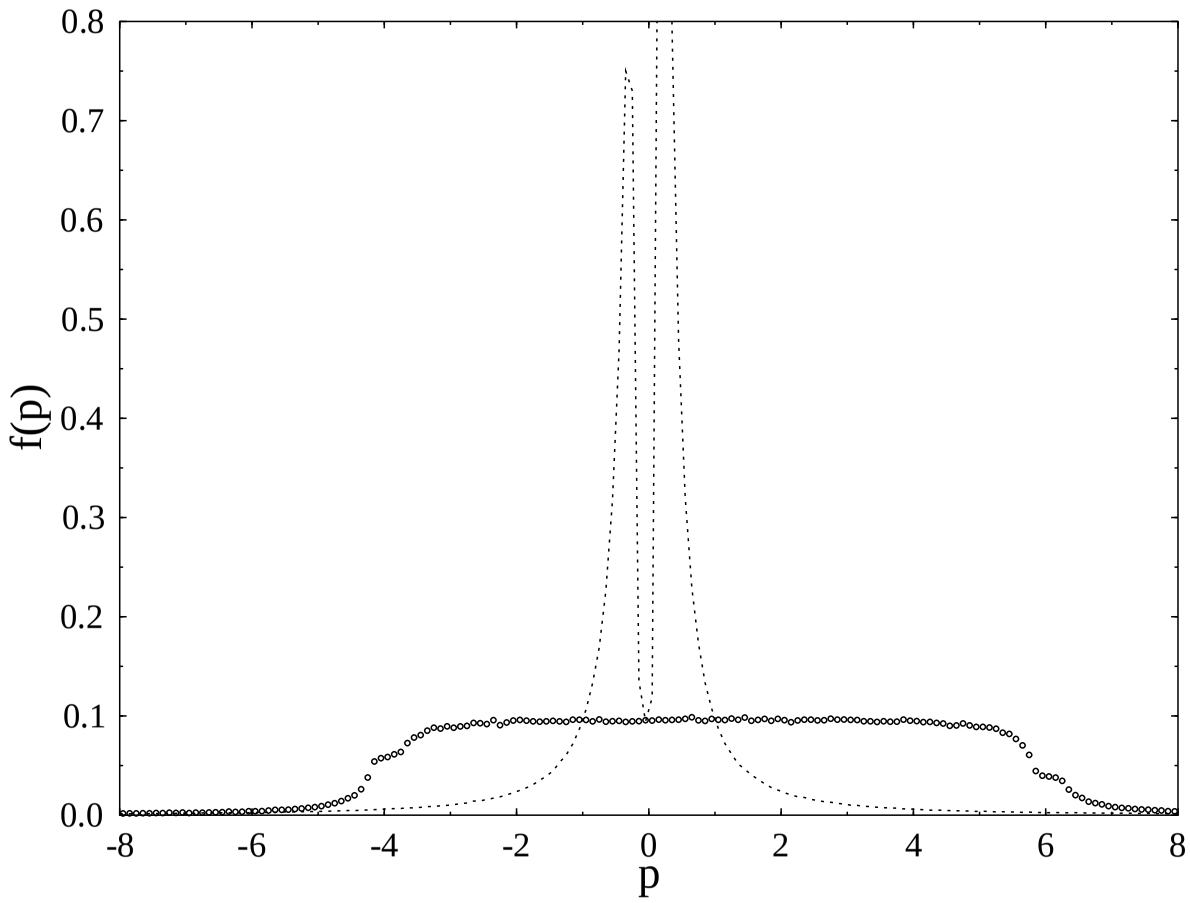

Fig.7

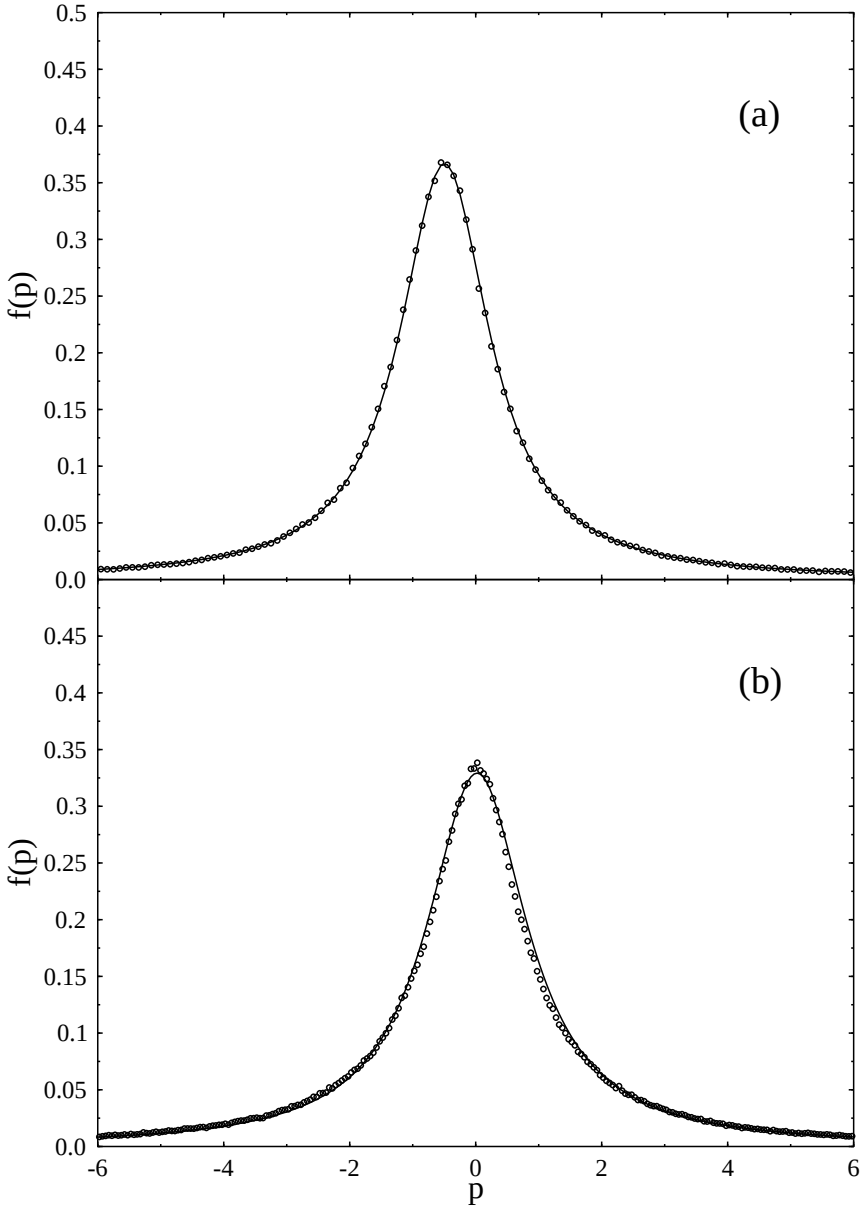

Fig.8